



## The MicroClimate Screen – A microscale climate exposure system for assessing the effect of CO<sub>2</sub>, temperature and UV on marine microalgae

Li Xie<sup>a,b</sup>, Ailbhe Macken<sup>a</sup>, Bjørn Johnsen<sup>c</sup>, Marit Norli<sup>a</sup>, Odd Arne Segtnan Skogan<sup>a</sup>, Knut Erik Tollefsen<sup>a,b,d,\*</sup>

<sup>a</sup> Norwegian Institute for Water Research (NIVA), Økernveien 94, N-0579, OSLO, Norway

<sup>b</sup> Norwegian University of Life Sciences (NMBU), Centre for Environmental Radioactivity, Post box 5003, N-1432, Ås, Norway

<sup>c</sup> Norwegian Radiation and Nuclear Safety Authority (DSA), Grini Næringspark 13, NO-1361, Østerås, Norway

<sup>d</sup> Norwegian University of Life Sciences (NMBU), Faculty of Environmental Sciences and Natural Resource Management, Post box 5003, N-1432, Ås, Norway

### ARTICLE INFO

#### Keywords:

Climate change  
Micro-scale exposure system  
Ocean acidification  
Temperature  
Ultraviolet radiation  
Diatom

### ABSTRACT

Global warming and anthropogenic activities are changing the ocean, inducing profound impacts on marine life and ecosystems from changing physical and chemical factors in and above the water column. Rising surface temperatures, ocean acidification, and seasonal variations in UV radiation (UVR), modulated by water clarity and sea-ice extent, affect life cycles of the marine food-web, and directly or indirectly also the global carbon fixation. Diatoms, pelagic microalgae that are responsible for 40% of the marine productivity, have limited capability to avoid exposure to changing ocean conditions, and hence, highly relevant for model studies of the influence of climate change on growth and productivity in the marine environment. A plate-based high-throughput exposure system was constructed to assess the biological effects from relevant climate change factors on the diatom *Skeletonema pseudocostatum*, conducted as a chronic toxicity tests over 72 h periods. The exposure system consisted of a micro-climate unit and a light-exposure unit, enabling accurate regulation of pCO<sub>2</sub>, temperature, UVR and photosynthetic active radiation (PAR). Changes in physical factors, including pH, dissolved inorganic carbon (DIC), total alkalinity (TA), temperature and salinity in the medium, as well as reduction in growth were characterised to demonstrate performance of the micro exposure system. The results demonstrate that the exposure system successfully simulated ocean acidification and could maintain stable temperature (CV < 3%), PAR and UVR irradiance (CV < 8%). Growth inhibition responses were typically dose-dependent and verified that the micro-exposure system could be used to assess effects and adaptations to climate-relevant stressors.

### 1. Introduction

Climate change has been predicted to alter the physical and chemical characteristics of the ocean in substantial ways over the next decades (Gregg and Rousseaux, 2016; Neale et al., 2021; Rousseaux and Gregg, 2015). The changing factors in marine environment such as increases in the concentration of dissolved CO<sub>2</sub>, sea surface temperature and solar ultraviolet radiation may cause profound effects in the structure and function of marine ecosystems (Hays et al., 2005). Generally, marine environmental conditions largely drive the physiological characteristics, diversity and abundance of primary producers, such as phytoplankton (Harley et al., 2006). Disturbances in the growth and reproduction of primary producers due to climate change can lead to a shift in the

growth of secondary plankton, ultimately affecting the structure of the marine food web. Additionally, changes in phytoplankton composition and productivity may also affect the marine biochemical cycling and global carbon fixation. As a consequence of increasing anthropogenic CO<sub>2</sub> emissions, the concentration of greater dissolved CO<sub>2</sub> is expected to lead to an increase in ocean acidification (OA), with an average pH decline of 0.002 pH units per year and a potential drop of 0.3–0.4 pH units by 2100 (Orr et al., 2005).

The effects of increased CO<sub>2</sub> concentrations on marine algae have been studied for years, and most of these studies addressed single stressors scenarios, with some notable exceptions (Mackey et al., 2015; Wu et al., 2014). To better understand the biological impacts of climate change, recent studies have started investigating the interaction

\* Corresponding author. Norwegian Institute for Water Research (NIVA), Section of Ecotoxicology and Risk Assessment, Økernveien 94, N-0579, OSLO, Norway.  
E-mail address: [knut.erik.tollefsen@niva.no](mailto:knut.erik.tollefsen@niva.no) (K.E. Tollefsen).

<https://doi.org/10.1016/j.marenvres.2022.105670>

Received 17 February 2022; Received in revised form 16 May 2022; Accepted 29 May 2022

Available online 16 June 2022

0141-1136/© 2022 The Authors. Published by Elsevier Ltd. This is an open access article under the CC BY license (<http://creativecommons.org/licenses/by/4.0/>).

between OA and other environmental factors, such as rising temperatures or UV radiation (Gao et al., 2018a, 2018b). Ocean acidification is not a solitary process but adds to a multitude of other climate-relevant factors. Hence, interactive effects, such as increased temperature and solar UV exposure needs to be comprehensively considered (Koch et al., 2013). During the 20th century, as a result of anthropogenic emission of greenhouse gases, ocean surface temperatures continually rising around the world. According to the National Oceanic and Atmospheric Administration (NOAA), global ocean surface temperatures in 2020 were 0.76 °C higher than the average of the 20th century, and the modelling studies predicted that the average global ocean temperature could rise 1–4 °C by 2100 (IPCC, 2013). Such increases in ocean surface temperature can impact marine ecosystems in several ways, such as altering plant-, animal- and microbial species abundance (i.e. population growth) and biodiversity, influencing reproduction capacity, migration patterns, frequency and intensity of harmful algal blooms (Neale et al., 2021). Additionally, seasonal enhancements in surface UVR, particularly at high latitudes (Bernhard et al., 2020), modulated by the timing of sea-ice coverage, clouds, and episodes of low atmospheric ozone amount in connection with strong and extensive polar vortices, may potentially have negative impacts on phytoplankton, fish eggs and larvae when they are in their most vulnerable life stages (Hader et al., 2007). UVB-induced inhibition of photosynthesis in phytoplankton has been demonstrated for Antarctic waters, and ozone-induced spectral shifts of in-water spectral irradiances may additionally alter the balance of spectrally dependent phytoplankton processes (Smith et al., 1992). Laboratory studies, using artificial light to simulate enhanced solar UV, have demonstrated various adverse effects on aquatic primary producers, including induction of oxidative stress, DNA damage, changes in photosynthesis, secondary metabolites and reproduction etc. (Pessoa, 2012; Xie et al., 2020). The Montreal Protocol and its amendments have been successful in mitigating destruction of the ozone layer, however, recent projections on long-lived halogen substances residing in the stratosphere suggests that conditions favourable for large seasonal ozone depletions in the Arctic may persist or even deteriorate until the end of this century, if future abundances of greenhouse gases continue to steeply increase (von der Gathen et al., 2021).

Hence, studies of the effects of UV radiation and climate change on marine ecosystems and biodiversity will be relevant for a longer perspective (Neale et al., 2021). To facilitate high-throughput assessment of effects from climate change on marine phytoplankton, a microscale (microplate-based) system integrated into traditional laboratory-based incubators was therefore designed to simulate scenarios of combined increased CO<sub>2</sub> uptake in sea-water, rising temperature and enhanced UVB exposure. The exposure system aimed to accurately control these abiotic and biotic factors, while maintaining high-throughput capacity of microplate bioassays. In the present study, the diatom *Skeletonema pseudocostatum* was used as a model organism. This diatom represents one of the most abundant algal species in coastal waters worldwide (Rousseaux and Gregg, 2015) and has been successfully used as an indicator of the ecological quality of aquatic ecosystems worldwide. This is due to its rapid reproduction rate, being well established in the food web, as well as being sensitive to the majority of physical, chemical and biological changes in water bodies (DeLorenzo et al., 2001). Changes in physical parameters, including pH, dissolved inorganic carbon (DIC), total alkalinity (TA), temperature and salinity in the medium were monitored, and growth responses of *S. pseudocostatum* characterised to assess adverse effects after exposure to UVR, increased temperature and partial pressure of CO<sub>2</sub> (pCO<sub>2</sub>).

## 2. Material and method

### 2.1. Micro-climate exposure system

The micro-climate exposure system consists of three micro-climate units that can be placed inside a lab-scale incubator, combined with a

UV and light exposure panel at the top. The micro-climate unit has a separate pre-equilibration gas system (gas cylinder and gas humidifier), and computer-controlled, temperature regulated exposure compartment. The micro-climate units (Fig. 1) were manufactured using UV transmitting plexiglass (8 mm PLEXIGLAS® GS 2458 SC, Röhm GmbH, Darmstadt, FRG). The incubator itself (Multitron-Pro incubator, Infors HT, Bottmingen, Switzerland) has an air cycling system, and an in-house-made computer-controlled heating system (programmed in Labview 2015; National Instruments, Austin, TX, USA) with heater (K010030C5-0009B, Watlow Polyimide, Missouri USA) and temperature sensor (LM35Z, NOPB, Texas, USA). The light exposure unit is a custom-made UV exposure chamber consisting of a Multitron-Pro incubator (Infors HT, Bottmingen, Switzerland), equipped with fluorescent tubes for the UVA (UV-A 36W/78, Centra Osram, Berlin, Germany, peak emission approximately 330 nm), UVB (PL-UV-B tubes (L 36W/UV-B UV6, Waldmann, Villingen-Schwenningen, Germany, peak emission approximately 310 nm) and PAR (Osram 36 W T8 Fluorescent T, OSRAM, Oslo, Norway). An inhouse light-regulating system based on MultiOne Configurator (version 2.7, Philips, Surrey, UK) was developed to separately control the intensity and light/darkness periods of UVB, UVA and PAR.

### 2.2. Stability tests

To validate the microscale chambers, three independent tests were conducted with different partial pressures of CO<sub>2</sub> (pCO<sub>2</sub>), temperatures and UV radiation.

#### 2.2.1. Increased CO<sub>2</sub>

The first stability test simulated the ocean acidification due to increased pCO<sub>2</sub> levels. Before exposure, the sea water was pre-equilibrated for 72h with 350, 500, 1000 ppm CO<sub>2</sub>, levels considered relevant for climate change scenarios for 1990, 2050 and 2100, respectively (Plattner et al., 2001). After pre-equilibration, sea water was sampled prior to the start of the experiment for dissolved inorganic carbon (DIC) using VINDTA 3C (Versatile Instrument for the Detection of Total Alkalinity, <http://www.marianda.com>) by coulometry (Dickson and Millero, 1987). Due to the limitation of the water volume in the bioassay, no replicates were used in the measurement after pre-equilibration. The pH was measured with a pH meter (SympHony SB70P, VWR, Belgium) that was calibrated daily with a standard National Bureau of Standards (NBS) buffer of pH 4.0, pH 7.0 and 10.0 (Sigma-Aldrich). Pre-equilibrated seawater was then transfer into the 12 well microplates and placed in the different micro-climate units with the different pCO<sub>2</sub> levels for 72h. The temperature and salinity were measured before and after exposure using a thermometer (M model, CoolProbe™, VWR, Belgium) and refractometer (ATAGO S/Mill hand refractometer), respectively. The pCO<sub>2</sub> and nutrients were computed with CO2SYS (V2.1.xls) software based on the known values of DIC, pH, salinity (Lewis and Wallace 2006). The dissociation constants K1 and K2 were defined according to Roy et al. (1996), and the KHSO<sub>4</sub> was taken from Dickson (1990).

#### 2.2.2. Increased temperature

The second stability study simulated a global warming scenario. An identical approach was undertaken for this study, although the exposures were now conducted at different temperatures (20 °C, 24 °C, 28 °C) and a constant CO<sub>2</sub> level (350 ppm). Algal medium (F/2 medium, detailed in section 2.3.1) was transfer into the 12 well microplates and the plates were placed in the three micro-climate units with these different temperature levels for 72h. The temperature, pH and salinity were measured before and after exposure using the thermometer (M model, CoolProbe™, VWR, Belgium), pH meter (SympHony SB70P) and refractometer (ATAGO S/Mill hand refractometer), respectively.

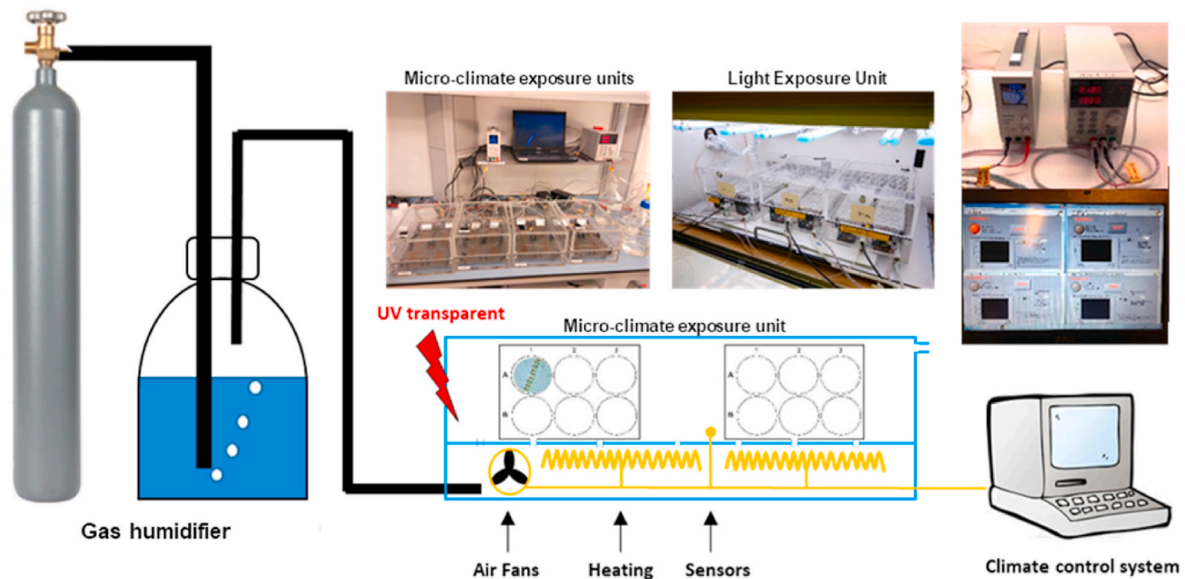


Fig. 1. Schematic representation of multiple stressors exposure unit, including micro-climate exposure units, light exposure unit and control system.

### 2.2.3. UV radiation

The third study targeted a validation of the light conditions inside the micro-climate units after they had been installed in the combined incubator and light exposure unit. Light conditions were measured outside and inside the micro-climate units under three different spectral irradiance regimes: non-UV control (PAR:  $100 \mu\text{mol m}^{-2} \text{s}^{-1}$ ), UV-A control (PAR:  $100 \mu\text{mol m}^{-2} \text{s}^{-1}$ , UV-A:  $4 \text{ W m}^{-2}$ , UV-B  $<0.008 \text{ W m}^{-2}$ ) and combined UV-B and UVA control (PAR:  $100 \mu\text{mol m}^{-2} \text{s}^{-1}$ , UV-A:  $4 \text{ W m}^{-2}$ , UV-B:  $0.5 \text{ W m}^{-2}$ ). The UV-A control was obtained with the lamps (PAR + UVA) covered with pre-burned (24 h exposed to  $1 \text{ W m}^{-2}$  UV-B) polyester foil (PT, 0.175 mm, Nordbergs Tekniska AB, Vallentuna Sweden) to effectively block radiation with wavelengths  $<315 \text{ nm}$ . Combined UVB and UVA radiation was obtained by covering the lamps (PAR + UVA + UVB) with pre-burned (24 h exposed to  $1 \text{ W m}^{-2}$  UV-B) cellulose acetate (CA, 0.13 mm, Jürgen Rachow, Hamburg, Germany), which completely absorbs wavelengths below the ozone-cutoff region of the solar spectrum (wavelengths  $<290 \text{ nm}$ ). The tests were conducted under constant temperature regulation ( $20^\circ\text{C}$ ) and  $\text{CO}_2$  level (350 ppm). UV transmittance spectra of the plexiglass (Supple. Fig. S1) was confirmed by measurements by the Norwegian Radiation and Nuclear Safety Authority (DSA, Oslo, Norway), applying a calibrated Bentham DTM300 high-resolution scanning spectroradiometer (Bentham DTM 300, Bentham Instruments Ltd, Reading, UK). PAR and UV irradiance inside and outside the exposure chambers were measured with a portable SpectroSense 2+ filter radiometer (Skye Instruments Ltd, Llandrindod Wells, UK), that had been calibrated against the same Bentham spectroradiometer.

## 2.3. Validation test with microalgae

### 2.3.1. Test organism

*Skeletonema pseudocostatum* (formerly *S. costatum* Cleve) was obtained from the Norwegian Culture Collection of Algae, NORCCA. (Strain NIVA-BAC 1). Algae were grown in F/2 medium in  $0.22 \mu\text{m}$  filtered natural seawater, which was enriched with  $3.0 \text{ mM KNO}_3$ ,  $0.1 \text{ mM Na}_2\text{HPO}_4$ ,  $70 \mu\text{M NaSiO}_3$ ,  $1.0 \mu\text{M FeSO}_4$  and  $25 \mu\text{M EDTA-Na}$  (Guillard and Ryther, 1962). Algal cultures were semi-continuously maintained by partial exchange of the culture media every 3 days in 500 ml flasks with the  $\text{CO}_2$ -equilibrated medium (350 ppm) and a 12 h:12 h light: dark cycle of illumination at  $100 \mu\text{mol photons m}^{-2} \text{s}^{-1}$  provided by cool white fluorescent tubes. The initial algae concentrations were adjusted to  $1 \times 10^6 \text{ cells ml}^{-1}$  and measured with a

Beckman-Coulter Multisizer 3 Coulter Counter (Miami, FL, US). Algae were cultured with 9 semi-continuous dilutions at identical conditions mentioned above to enable full acclimation and stable growth rates to the exposure conditions used in subsequent experiments.

### 2.3.2. Exposure

Validation tests were carried out in conjunction with stability tests of  $\text{pCO}_2$ . To evaluate the effects of increased  $\text{CO}_2$  on *S. pseudocostatum*, 72h growth inhibition tests were performed according to the ISO standard ISO10253:2016 (ISO, 2016). For the  $\text{pCO}_2$  test, the medium was pre-equilibrated with  $\text{CO}_2$  as described above in the stability test (Section 2.2.1). Algae were then diluted with pre-equilibrated medium and transferred into 12-well microplates and placed inside the micro-climate units aerated with different  $\text{CO}_2$  levels (350, 500, 1000 ppm) and exposed for 72h. For the temperature test, three levels of temperature ( $20^\circ\text{C}$ ,  $24^\circ\text{C}$ ,  $28^\circ\text{C}$ ) with a constant  $\text{CO}_2$  level (350 ppm) were set in different chambers as described in the stability test (Section 2.2.2) and *S. pseudocostatum* exposed for 72 h.

To implement the different UV regimes, three different light treatments (Non-UV, UVA and UVB) were set in different climate chambers with a constant temperature and  $\text{CO}_2$  level as described above (section 2.2.3) and *S. pseudocostatum* exposed for 72 h. The exposure was conducted in the light exposure unit with orbital shaking at 90 rpm, continuous PAR of  $100 \mu\text{mol m}^{-2} \text{s}^{-1}$  and a temperature of  $20^\circ\text{C}$ . After exposure, algal growth was measured by fluorescence using a Cytofluor 2300 (Millipore, Billerica, MA, US) with excitation and emission fluorescence at 530 nm and 685 nm, respectively (Petersen et al., 2014). Growth was also measured at time 0 h in the same manner prior to the exposure. The growth rate was then calculated from initial fluorescence and fluorescence after exposure using the equation:

$$\mu = \frac{\ln(N_n) - \ln(N_0)}{t_n} \times 24 \text{ d}^{-1}$$

where  $N_n$  is the fluorescence at time at  $t_n$ ,  $N_0$  is the initial fluorescence at time zero.  $t_n$  is the exposure time (h).

### 2.4. Statistics

All statistical and graphical analysis were conducted in GraphPad Prism version 8 (GraphPad Software, La Jolla, California, USA). The Shapiro-Wilk test was used to check the normal distribution. Differences between controls and treated samples were analyzed by one-way

ANOVA followed by Dunnett's multiple comparison test using a threshold of  $p < 0.05$  for significance.

### 3. Results and discussion

#### 3.1. Validation of multiple stressors exposure system

##### 3.1.1. Water chemical analysis

After pre-equilibrating, the pH values in the medium measured 8.18, 8.04 and 7.78 for CO<sub>2</sub> levels of 350, 500 and 1000 ppm, respectively. In addition to this, the computed results showed that elevated CO<sub>2</sub> levels led to an increase in pCO<sub>2</sub> and carbonate system components (dissolved CO<sub>2</sub> (aqCO<sub>2</sub>)) and HCO<sub>3</sub><sup>-</sup> and CO<sub>3</sub><sup>2-</sup> in pre-equilibrated seawater (Table 1 and Table S1). This suggests that the micro-climate units successfully simulated ocean acidification conditions predicted to be induced by increased atmospheric CO<sub>2</sub>. Additionally, an 8% increase in DIC was also observed in the medium after pre-equilibrating, while slight change (2%) in TA was observed (Table 1). These results are in agreement with the observation from other seawater carbonate systems, where increased CO<sub>2</sub> (1000 ppm) caused no change in TA in F/2 medium, but strongly enhanced the DIC and reduced the pH (Yuan et al., 2018).

##### 3.1.2. Temperature and salinity control

In the stability studies with different CO<sub>2</sub> levels, temperature was controlled with less than 3% deviation between nominal and actual temperatures, and no significant changes in water temperature were observed before and after exposure (Fig. 2. A). Stable temperature control under different temperature conditions was also observed in the temperature study (Fig. 2. C). The evaporation rate of seawater in the microplates inside the exposure chamber was also acceptable, as the change in salinity was less than 5% in both studies (Fig. 2. B and D). The results suggest that the exposure system can effectively simulate the global warming caused by increasing atmospheric CO<sub>2</sub> concentrations and pCO<sub>2</sub> in seawater.

##### 3.1.3. UV exposure conditions

The UVB irradiance (0.5 Wm<sup>-2</sup>) used in the UV exposure experiments simulated clear sky seasonal noon UVB irradiance at a coastal area in southern Norway (Landvik 58°N, Norway) in early spring (DSA, 2020). While the emission spectrum of fluorescent UVB tubes is overlapping with the UVA region and only long-pass filters (CA filter) were available, contributions from wavelengths in the UVA could not be fully excluded, however kept as low as possible by choosing a lamp with peak emission in the UVB part. However, separate experiments with UVA lamps, blocking the UVB contributions with long-pass filters (PT filter) served as a UVA control. Measurements with the portable radiometer indicated that the micro-climate exposure system enabled stable PAR, UVA and UVB irradiances inside the chambers (Fig. 3), which is in agreement with the UVB transmittance results (Supple. Fig. S1).

#### 3.2. Validation test with microalgae

An initial validation of the test system was conducted to simulate an ocean acidification scenario, global warming and increased background level of UV radiation. In the validation studies, the model diatom *S. pseudocostatum* was exposed to three different CO<sub>2</sub> levels,

**Table 1**

Change of pH, dissolved inorganic carbon (DIC) and computed total alkalinity (TA) and pCO<sub>2</sub> in pre-equilibrated sea water with different CO<sub>2</sub> levels.

CO <sub>2</sub> (ppm)	pCO <sub>2</sub> (ppm)	pH	DIC (μmol L <sup>-1</sup> )	TA (μmol L <sup>-1</sup> )
350	283	8.18	2030	2370
500	423	8.04	2125	2383
1000	816	7.78	2193	2328

temperatures, and light conditions, respectively. Changes of pH under different CO<sub>2</sub> levels before and after exposure were summarized in Table S2. After 72h exposure, apparent increase of pH (2%) was observed in the diatom medium, suggesting that the growth of the diatom also affected the pH in seawater. The increase in pH is likely to be associated with the photosynthesis of *S. pseudocostatum* during the exposure, which removed dissolved CO<sub>2</sub> from the water and increasing the pH (Chen and Durbin, 1994). The growth rates of *S. pseudocostatum* was analyzed and compared to other studies. The results indicated that the elevated CO<sub>2</sub> level significantly enhanced the growth of *S. pseudocostatum* at 500 ppm, while no significant effects were observed at 1000 ppm (Fig. 4. A). The results were consistent with previous findings where increased growth was observed in several diatoms after exposure to increased CO<sub>2</sub> (Bach and Taucher, 2019; Wu et al., 2010). Additionally, no significant changes were observed on the growth rates of the *S. pseudocostatum* when exposed 20, 24 and 28 °C, respectively (Fig. 4. B). This result is consistent with the observation that an increase in temperature from 20 °C to 30 °C did not change the growth rate of *S. pseudocostatum* (Ebrahimi and Salarzadeh, 2016). When exposed to different UV-regimes, PAR + UVA caused no relevant change on *S. pseudocostatum* growth compared to the non-UV control (PAR), while a 30% reduction in growth was observed in the PAR + UVA + UVB treatment (Fig. 4. C). The latter observation agrees well with previous studies showing that 3 days exposure to UVA radiation (28 W m<sup>-2</sup>) did not cause any significant effects on *S. pseudocostatum* compared to PAR alone (Wu et al., 2009). Growth inhibition induced by UVB radiation is also observed in field studies where the growth of *S. pseudocostatum* decreased by 29% after 5 days exposure to UVB at 0.78 W m<sup>-2</sup> (Gao et al., 2009). The consistent results suggested this micro-climate chamber provided a good simulation of the effects of different types of climate changes on diatoms.

### 4. Conclusion

The presented study validated the in-house microscale screening system using classical toxicity studies with diatom *S. pseudocostatum*. The results demonstrated the utility of the micro-climate exposure system for studying the effects of climate change, including increased temperature, UV radiation and pCO<sub>2</sub> levels. Moreover, such micro-scale sized exposure system is anticipated to also support studies of relevant environmental stressors such as temperature (global warming), non-ionizing radiation (e.g. UVA and UVB radiation), ionizing radiation (e.g. alpha, beta, gamma and x-ray radiation) and chemical stressors (inorganic and organic stressors) alone and in combinations to support future studies with a larger array of phyto- and zooplankton. Additional studies will be conducted to also evaluate physiological responses to enhance mechanistical understanding of single and multiple stressor effects by predicted near and distant future global change scenarios.

#### Conflict of interest and authorship conformation form

The authors declared that.

- All authors have participated in (a) conception and design, or analysis and interpretation of the data; (b) drafting the article or revising it critically for important intellectual content; and (c) approval of the final version.
- This manuscript has not been submitted to, nor is under review at, another journal or other publishing venue.
- The authors have no affiliation with any organization with a direct or indirect financial interest in the subject matter discussed in the manuscript
- The following authors have affiliations with organizations with direct or indirect financial interest in the subject matter discussed in the manuscript:

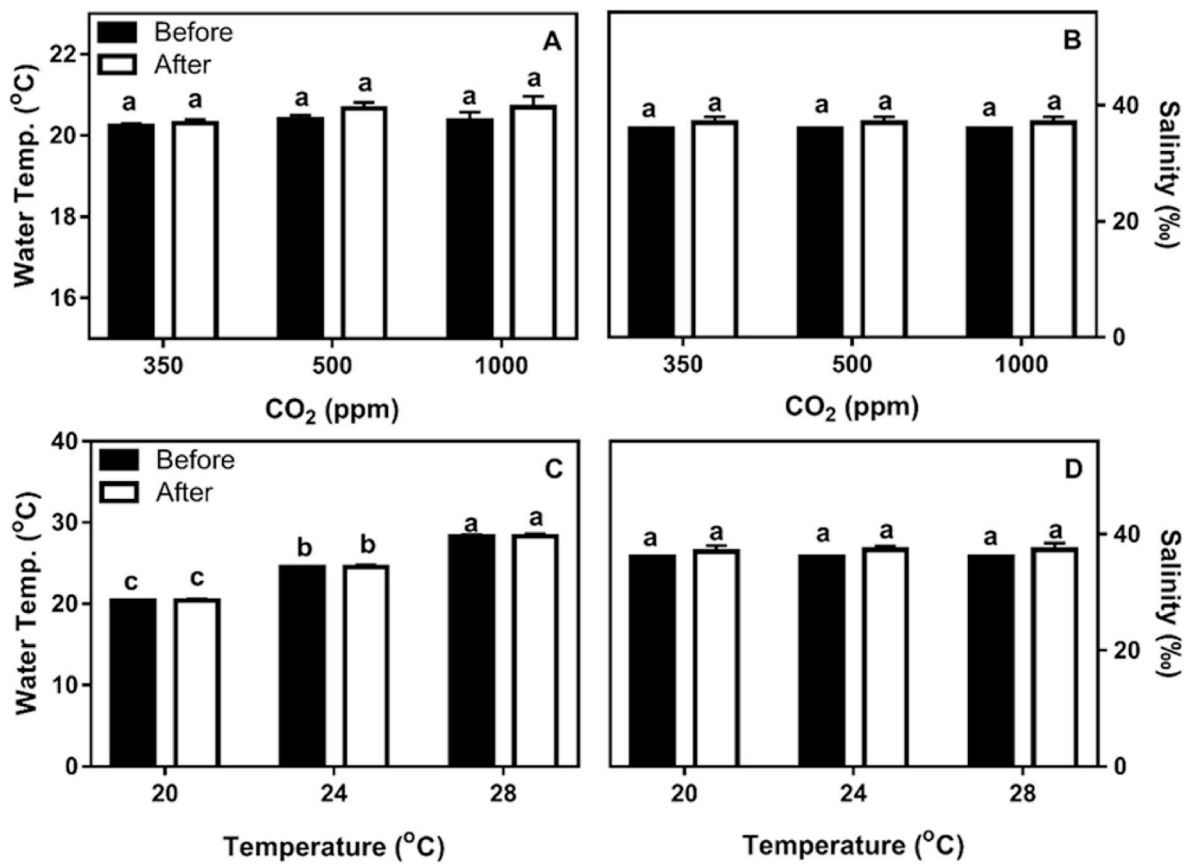


Fig. 2. Change of water temperature and salinity under different levels of CO<sub>2</sub> and temperature. The letters indicate differences between treatments (Mean of 3 replicates ± SE).

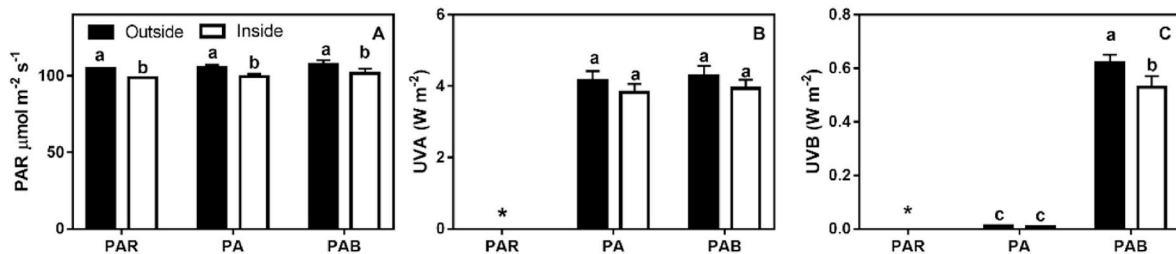


Fig. 3. Intensity of PAR (A), UVA radiation (B) and UVB radiation (C) outside and inside the micro-climate chamber when exposed for PAR (Non-UV), PA (PAR + UVA) and PAB (PAR + UVA + UVB). The letters indicate differences between treatments ( $P \leq 0.05$ ). The asterisk “\*” refers to the intensity of UVA and UVB were too low to be detected.

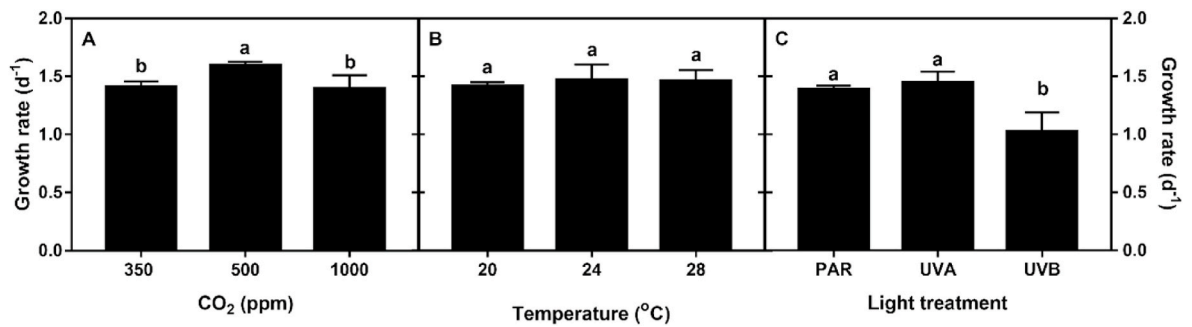


Fig. 4. Growth rates of *Skeletonema pseudocostatum* after exposure to different level of CO<sub>2</sub> (A), temperatures (B) and light conditions (C). The letters indicate differences between treatments ( $P \leq 0.05$ ).

## Declaration of competing interest

The authors declare the following financial interests/personal relationships which may be considered as potential competing interests:

The following authors have affiliations with organizations with direct or indirect financial interest in the subject matter discussed in the manuscript:

Author's name Affiliation.

Li Xi Norwegian Institute for Water Research.

Ailbhe Macken Norwegian Institute for Water Research.

Marit Norli Norwegian Institute for Water Research.

Bjørn Johnse Norwegian Radiation and Nuclear Safety Authority.

Odd Arne Segtnan Skogan Norwegian Institute for Water Research.

Knut Erik Tollefsen Norwegian Institute for Water Research.

## Acknowledgements

This study was supported by the Research Council of Norway (RCN) through the Norwegian Institute for Water Research basic funding (SIS-program on Ocean Acidification, RCN contract number 160016), the Centres of Excellence (CoE) funding scheme (RCN contract number 223268), and the NIVA Computational Toxicology Program, NCTP ([www.niva.no/nctp](http://www.niva.no/nctp)). The skilful assistance of Hans Christian Tollefsen in constructing the light controlling systems is also acknowledged.

## Appendix A. Supplementary data

Supplementary data to this article can be found online at <https://doi.org/10.1016/j.marenvres.2022.105670>.

## References

- Bach, L.T., Taucher, J., 2019. CO<sub>2</sub> effects on diatoms: a synthesis of more than a decade of ocean acidification experiments with natural communities. *Ocean Sci.* 15 (4), 1159–1175. <https://doi.org/10.5194/os-15-1159-2019>.
- Bernhard, G.H., Fioletov, V.E., Ju, Grooss, Ialongo, I., Johnsen, B., Lakkala, K., Manney, G.L., Muller, R., Svendby, T., 2020. Record-breaking increases in arctic solar ultraviolet radiation caused by exceptionally large ozone depletion in 2020. *Geophys. Res. Lett.* 47 (24) <https://doi.org/10.1029/2020gl090844>.
- Chen, C.Y., Durbin, E.G., 1994. Effects of pH on the growth and carbon uptake of marine phytoplankton. *Mar. Ecol. Prog. Ser.* 109 (1), 83–94. <https://doi.org/10.3354/meps109083>.
- DeLorenzo, M.E., Scott, G.L., Ross, P.E., 2001. Toxicity of pesticides to aquatic microorganisms: a review. *Environ. Toxicol. Chem.* 20 (1), 84–98. <https://doi.org/10.1002/etc.5620200108>.
- Dickson, A.G., 1990. Standard potential of the reaction: AgCl(s) + 1/2H<sub>2</sub>(g) = Ag(s) + HCl(aq), and the standard acidity constant of the ion HSO<sub>4</sub><sup>-</sup> in synthetic sea water from 273.15 to 318.15 K. *J. Chem. Thermodyn.* 22 (2), 113–127. [https://doi.org/10.1016/0021-9614\(90\)90074-z](https://doi.org/10.1016/0021-9614(90)90074-z).
- Dickson, A.G., Millero, F.J., 1987. A comparison of the equilibrium constants for the dissociation of carbonic acid in seawater media. *Deep-Sea Res., Part A* 34 (10), 1733–1743. [https://doi.org/10.1016/0198-0149\(87\)90021-5](https://doi.org/10.1016/0198-0149(87)90021-5).
- Ebrahimi, E., Salarzadeh, A., 2016. The effect of temperature and salinity on the growth of *Skeletonema costatum* and *Chlorella capsulata* in vitro. *Int. J. Life Sci.* 10, 40. <https://doi.org/10.3126/ijls.v10i1.14508>.
- Gao, G., Gao, K.S., Giordano, M., 2009. Responses to solar UV radiation of the diatom *Skeletonema costatum* (Bacillariophyceae) grown at different Zn<sup>2+</sup> concentrations. *J. Phycol.* 45 (1), 119–129. <https://doi.org/10.1111/j.1529-8817.2008.00616.x>.
- Gao, G., Shi, Q., Xu, Z.G., Xu, J.T., Campbell, D.A., Wu, H.Y., 2018a. Global warming interacts with ocean acidification to alter PSII function and protection in the diatom *Thalassiosira weissflogii*. *Environ. Exp. Bot.* 147, 95–103. <https://doi.org/10.1016/j.envexpbot.2017.11.014>.
- Gao, G., Xu, Z.G., Shi, Q., Wu, H.Y., 2018b. Increased CO<sub>2</sub> exacerbates the stress of ultraviolet radiation on photosystem II function in the diatom *Thalassiosira weissflogii*. *Environ. Exp. Bot.* 156, 96–105. <https://doi.org/10.1016/j.envexpbot.2018.08.031>.
- Gregg, W.W., Rousseaux, C.S., 2016. Directional and spectral irradiance in ocean models: effects on simulated global phytoplankton, nutrients, and primary production. *Front. Mar. Sci.* 3 <https://doi.org/10.3389/fmars.2016.00240>.
- Guillard, R.R.L., Ryther, J.H., 1962. Studies of marine planktonic diatoms. I. *Cyclotella nana* Hustedt, and *Detonula confervacea* (Cleve) Gran. *Can. J. Microbiol.* 8 (2), 229–239. <https://doi.org/10.1139/m62-029>.
- Hader, D.P., Kumar, H.D., Smith, R.C., Worrest, R.C., 2007. Effects of solar UV radiation on aquatic ecosystems and interactions with climate change. *Photochem. Photobiol. Sci.* 6 (3), 267–285. <https://doi.org/10.1039/b700020k>.
- Harley, C.D.G., Hughes, A.R., Hultgren, K.M., Miner, B.G., Sorte, C.J.B., Thornber, C.S., Rodriguez, L.F., Tomanek, L., Williams, S.L., 2006. The impacts of climate change in coastal marine systems. *Ecol. Lett.* 9 (2), 228–241. <https://doi.org/10.1111/j.1461-0248.2005.00871.x>.
- Hays, G.C., Richardson, A.J., Robinson, C., 2005. Climate change and marine plankton. *Trends Ecol. Evol.* 20 (6), 337–344. <https://doi.org/10.1016/j.tree.2005.03.004>.
- Koch, M., Bowes, G., Ross, C., Zhang, X.H., 2013. Climate change and ocean acidification effects on seagrasses and marine macroalgae. *Global Change Biol.* 19 (1), 103–132. <https://doi.org/10.1111/j.1365-2486.2012.02791.x>.
- Lewis, D.E., Wallace, D.W.R., 2006. MS Excel Program Developed for CO<sub>2</sub> System Calculations. ORNL/CDIAC-105a. Carbon Dioxide Information Analysis Center. Oak Ridge National Laboratory, U.S. Department of Energy, Oak Ridge, Tennessee. [https://doi.org/10.3334/CDIAC/otg.CO2SYS\\_XLS.CDIAC105a](https://doi.org/10.3334/CDIAC/otg.CO2SYS_XLS.CDIAC105a).
- Mackey, K.R.M., Morris, J.J., Morel, F.M.M., Kranz, S.A., 2015. Response of photosynthesis to ocean acidification. *Oceanography* 28 (2), 74–91. <https://doi.org/10.5670/oceanog.2015.33>.
- Neale, R.E., Barnes, P.W., Robson, T.M., Neale, P.J., Williamson, C.E., Zepp, R.G., Wilson, S.R., Madronich, S., Andradý, A.L., Heikkilä, A.M., Bernhard, G.H., Bais, A. F., Aucamp, P.J., Banaszak, A.T., Bornman, J.F., Bruckman, L.S., Byrne, S.N., Foererd, B., Hader, D.P., Hollestein, L.M., Hou, W.C., Hylander, S., Jansen, M.A.K., Klekociuk, A.R., Liley, J.B., Longstreth, J., Lucas, R.M., Martinez-Abaigar, J., McNeill, K., Olsen, C.M., Pandey, K.K., Rhodes, L.E., Robinson, S.A., Rose, K.C., Schikowski, T., Solomon, K.R., Sulzberger, B., Ukpebor, J.E., Wang, Q.W., Wangberg, S.A., White, C.C., Yazar, S., Young, A.R., Young, P.J., Zhu, L., Zhu, M., 2021. Environmental effects of stratospheric ozone depletion, UV radiation, and interactions with climate change: UNEP Environmental Effects Assessment Panel, Update 2020. *Photochem. Photobiol. Sci.* 20 (1), 1–67. <https://doi.org/10.1007/s43630-020-00001-x>.
- Orr, J.C., Fabry, V.J., Aumont, O., Bopp, L., Doney, S.C., Feely, R.A., Gnanadesikan, A., Gruber, N., Ishida, A., Joos, F., Key, R.M., Lindsay, K., Maier-Reimer, E., Matear, R., Monfray, P., Mouchet, A., Najjar, R.G., Plattner, G.K., Rodgers, G.B., Rose, C.L., Sarmiento, J.L., Schlitzer, R., Slater, R.D., Totterdell, I.J., Weirig, M.F., Yamanaka, Y., Yool, A., 2005. Anthropogenic ocean acidification over the twenty-first century and its impact on calcifying organisms. *Nature* 437 (7059), 681–686. <https://doi.org/10.1038/nature04095>.
- Pessoa, M., 2012. Harmful effects of UV radiation in Algae and aquatic macrophytes – a review. *Emir. J. Food Agric.* 24, 510–526. <https://doi.org/10.9755/efja.v24i6.510526>.
- Petersen, K., Heiaas, H.H., Tollefsen, K.E., 2014. Combined effects of pharmaceuticals, personal care products, biocides and organic contaminants on the growth of *Skeletonema pseudocostatum*. *Aquat. Toxicol.* 150, 45–54. <https://doi.org/10.1016/j.aquatox.2014.02.013>.
- Plattner, G.K., Joos, F., Stocker, T.F., Marchal, O., 2001. Feedback mechanisms and sensitivities of ocean carbon uptake under global warming. *Tellus Ser. B Chem. Phys. Meteorol.* 53 (5), 564–592. <https://doi.org/10.1034/j.1600-0889.2001.530504.x>.
- Rousseaux, C.S., Gregg, W.W., 2015. Recent decadal trends in global phytoplankton composition. *Global Biogeochem. Cycles* 29 (10), 1674–1688. <https://doi.org/10.1002/2015gb005139>.
- Roy, R.N., Roy, L.N., Vogel, K.M., PorterMoore, C., Pearson, T., Good, C.E., Millero, F.J., Campbell, D.M., 1996. The dissociation constants of carbonic acid in seawater at salinities 5 to 45 and temperatures 0 to 45 degrees C (vol 44, pg 2499). *Mar. Chem.* 52 (2), 183. [https://doi.org/10.1016/0304-4203\(96\)83094-5](https://doi.org/10.1016/0304-4203(96)83094-5), 183.
- Smith, R.C., Prezelin, B.B., Baker, K.S., Bidigare, R.R., Boucher, N.P., Coley, T., Karentz, D., Macintyre, S., Matlick, H.A., Menzies, D., Ondrusek, M., Wan, Z., Waters, K.J., 1992. Ozone depletion: ultraviolet radiation and phytoplankton biology in antarctic waters. *Science* 255 (5047), 952–959. <https://doi.org/10.1126/science.1546292>.
- von der Gathen, P., Kivi, R., Wohltmann, I., Salawitch, R.J., Rex, M., 2021. Climate change favours large seasonal loss of Arctic ozone. *Nat. Commun.* 12 (1) <https://doi.org/10.1038/s41467-021-24089-6>.
- Wu, H.Y., Gao, K.S., Wu, H.Y., 2009. Responses of a marine red tide alga *Skeletonema costatum* (Bacillariophyceae) to long-term UV radiation exposures. *J. Photochem. Photobiol., B* 94 (2), 82–86. <https://doi.org/10.1016/j.jphotobiol.2008.10.005>.
- Wu, Y., Gao, K., Riebesell, U., 2010. CO<sub>2</sub>-induced seawater acidification affects physiological performance of the marine diatom *Phaeodactylum tricornutum*. *Biogeosciences* 7 (9), 2915–2923. <https://doi.org/10.5194/bg-7-2915-2010>.
- Wu, Y., Campbell, D.A., Irwin, A.J., Suggett, D.J., Finkel, Z.V., 2014. Ocean acidification enhances the growth rate of larger diatoms. *Limnol. Oceanogr.* 59 (3), 1027–1034. <https://doi.org/10.4319/lo.2014.59.3.1027>.
- Xie, L., Solhaug, K.A., Song, Y., Johnsen, B., Olsen, J.E., Tollefsen, K.E., 2020. Effects of artificial ultraviolet B radiation on the macrophyte *Lemma minor*: a conceptual study for toxicity pathway characterization. *Planta* 252 (5). <https://doi.org/10.1007/s00425-020-03482-3>.
- Yuan, W.B., Gao, G., Shi, Q., Xu, Z.G., Wu, H.Y., 2018. Combined effects of ocean acidification and warming on physiological response of the diatom *Thalassiosira pseudonana* to light challenges. *Mar. Environ. Res.* 135, 63–69. <https://doi.org/10.1016/j.marenvres.2018.01.016>.